A METHOD FOR RAPID ANALYSIS OF BIOFILM MORPHOLOGY AND COVERAGE ON GLASS AND POLISHED AND BRUSHED STAINLESS STEEL

A. Lomander, P. Schreuders, E. Russek-Cohen, L. Ali

Article was submitted for review in July 2001; approved for publication by the Biological Engineering Division of ASAE in January 2002.

The authors are **Andrea Lomander**, M.S., and **Paul D. Schreuders**, Ph.D., Assistant Professor, Biological Resources Engineering Department, University of Maryland, College Park, Maryland; **Estelle Russek-Cohen**, Ph.D., Professor, Animal and Avian Sciences Department, University of Maryland, College Park, Maryland; and **Laila H. Ali**, Ph.D., Senior Research Scientist, Division of Product Manufacture and Use, Office of Premarket Approval, Center for Food Safety and Applied Nutrition, Food and Drug Administration, Washington, D.C. **Corresponding author**: Paul D. Schreuders, Biological Resources Engineering Dept., University of Maryland, College Park, MD 20742; phone: 301-405-0145; fax: 301-314-9023; e-mail: ps129@umail.umd.edu.

ABSTRACT. *A tool for the rapid analysis of biofilms, using epifluorescence microscopy and image analysis was developed. The tool allows the evaluation of overall biofilm coverage and biofilm patch morphology. It will provide a quantitative method for identifying relationships between biofilms and their substrates and for identifying the morphology of patches of damaged bacteria. The coverage percentage allows evaluation of the growth of biofilms and will allow the evaluation of the effectiveness of sanitizers and mechanical cleaning methods in removing biofilms from food processing surfaces. The patch morphology is useful for investigating the relationships between surface morphology and biofilm growth and for determining the surface morphology, biofilm shape, and sanitizer effectiveness. The software was tested and validated using biofilms of* E. coli *K12 on glass, polished 316 stainless steel, and brushed 316 stainless steel. The biofilms were stained with both propidium iodide and SYTO-16. After performing digital image analysis of both overall coverage and biofilm patch morphometrics, it was found that the percentages of living or total biofilm were independent of the substrate material. However, the absolute area of individual biofilm patches varied depending on the substrate material. These areas also showed changes over time. The circularity of the biofilm patches was investigated. At the end of the studies, the shape of most of the biofilm patches in this group was nearly circular.*

Keywords. *Biofilms, Glass, 316 stainless steel, Morphometrics, Image analysis.*

It is well known that bacteria adhere to many surfaces involved in food processing and storage. The time required for bacteria to attach to surfaces and form hazardous biofilms can be as short as a few hours. A biofilm can be defined as matrix-enclosed bacteria populations adhering to one another and/or to surfaces or interfaces. A biofilm may uniformly cover its substrate or it may be quite "patchy." Biofilms may consist of only a monolayer of cells or be multilayered as thick as 300-400 μm (Costerton et al., 1994). The attachment of only a few species of bacteria may lead to the formation of a complex and diverse biofilm. Cells associated with biofilms have definite growth and survival advantages over planktonic cells. The exopolysaccharide matrix that surrounds the biofilm protects it from attack, and supplies it with nutrients (Costerton et al., 1994). This protective effect includes an increased resistance to sanitizers (James et al., 1995). The attachment of bacteria to a surface is active or passive depending on the motility of the bacteria. It also depends on diffusion and fluid forces from the surrounding fluid phase (Kumar and Anand, 1998). Further, adhesive substances on the surface of the cell, such as proteins, lipopolysaccharides, or flagella, govern the bacterial adhesion (Marshall, 1984). In irreversible adhesion, polymeric fibrils form a bridge between the bacterium and its substrate. Hence, there is a strong association between the bacteria and surface (Fletcher, 1996).

Many approaches to investigating biofilms concentrate on the disruption of the biofilm by scraping and evaluation of the growth of the recovered material on agar plates (Camper et al., 1996). This results in the elimination of essential features such as the biofilms' complex structure and organization (Wilkinson, 1998).

Observation of microorganisms in their natural habitat is best achieved with microscopic examination. However, most food-contact materials are opaque, limiting the use of transmitted light microscopy. Fluorescent staining of a biofilm and epifluorescence microscopic investigation avoids these limitations. The technique has been used for the evaluation of biofilms on food processing surfaces (Wirtanen and Mattila-Sandholm, 1993). In epifluorescence microscopy, the excitation light passes through the objective, excites the fluorophore, and the emitted light is collected by the objective for imaging. Several methods for analyzing these images have been reported. Yang et al. (2000) discuss the heterogeneity and texture of biofilms; Escher and Characklis (1988) used image analysis for a kinetic analysis of biofilms; while Kuehn et al. (1998) used semiautomated image analysis for analysis of biofilms in three dimensions.

We have developed a method that analyzes epifluorescence micrographs as a rapid tool for assessing the growth of biofilms on different surfaces. Since each bacterial strain has a different growth rate and many different strains form biofilms, it is important to be able to perform rapid two-dimensional estimation of a biofilm coverage and to get information regarding the biofilms' preference of surface material and surface structure. During this development, a non-pathogenic bacterial strain that is known to form thin biofilms on abiotic materials was desired, since thin biofilms would provide clearer images for analysis in two dimensions (Danese et al., 2000). The laboratory strain *E. coli* K12 met these requirements. The use of a non-starved medium further minimized the growth of thick biofilms (Dewanti and Wong, 1995). While the bacterial strain used in this study does not present a hazard to the food processing industry, the methods of analysis that are presented allow the identification of even small numbers of living or dead pathogens and can be applied to hazardous as well as innocuous bacteria. Our study investigated the morphology of the biofilm patches and their overall growth on three different surfaces: glass (G), polished 316 stainless steel (PSS), and brushed 316 stainless steel (BSS). Both glass and stainless steel are commonly used in the preparation and display of foods (Hood and Zottola, 1995, 1997). In addition, a model system was developed in which the bacterial colonies and the biofilm can be examined while still present on the chosen material.

MATERIALS AND METHODS

BIOFILM CULTURE

Bacterial Strain

E. coli K12 (Nutrition and Food Sciences Department, University of Maryland) was transferred to plates containing tryptic soy broth (TSB) and agar (both from VWR Scientific Products, West Chester, Pa.). The culture was maintained by plating it onto new TSB agar at regular intervals. All bacterial cultures were maintained in an incubator at 30°C.

Preparation of Billets

The biofilms were grown on surfaces prepared from 25 × 75 mm billets. Two materials (glass and 316 stainless steel) and two surface finishes of the stainless steel (polished to a bright finish, and brushed to a 2B roughness; Carnegie-Illinois, 1947) were considered. For the glass billets, soda lime glass microscope slides (Corning, Acton, Mass.) were used. The stainless steel billets were prepared from a single sheet of 316 stainless steel. To achieve a polished surface, the stainless steel billets were buffed prior to each experiment. The "brushed" billets were brushed to a matte finish with a stainless steel wire brush. After preparation, the billets were washed in acetone to remove residual oils and buffing compound.

Biofilm Culture Tanks

The development of biofilm growth in a circulating medium has been previously examined (Camper et al., 1996; Sternberg et al., 1999; Tolker-Nielsen et al., 2000). In our study, the biofilm culture tanks were manufactured from 13.6-liter polyethylene containers (VWR Scientific Products, West Chester, Pa.). In order to minimize localized nutrient depletion, the medium was circulated through the tank through a pair of holes in each of the long sides of the containers. Food-grade tubing (Norprene, Cole-Parmer, Vernon Hills, Ill.) attached to a peristaltic pump (Masterflex, Cole-Parmer, Vernon Hills, Ill.) was used to pump the medium. Stainless steel and glass billets were randomly inserted into a polycarbonate plate containing channels with a 2 cm spacing. The assembled apparatus was autoclaved prior to use. Throughout the study, the tanks were kept at 30°C.

Generation of Biofilms

Bacteria were cultured overnight on four TSB agar plates. The resulting colonies of bacteria were then transferred to a 500-mL culture flask containing 230 mL of sterile TSB. The flask and its contents were incubated on an Orbitron rotator at 30°C overnight. At the start of each experiment, the contents of the flask and 4.5 to 5.5 liters of additional sterile TSB medium were added to fill the tank. A pump rate of 200 to 220 mL/min ensured circulation of the medium. In the first group of experiments, pairs of tanks were maintained in the same incubator connected to two different pump heads. In the second group, the tanks were in two different incubators, and two different pumps were used.

Hemocytometer counts of the planktonic bacteria in the tank were performed according to Sieracki and Viles (1998) to determine the bacterial concentration. The initial planktonic bacterial concentration in the tank was 10^3 to 10^4 cells/mL medium. At the end of the experiments, the concentration was approximately 10^6 cells/mL medium. The viability counts were performed in order to ensure that the number of viable bacteria did not decrease. The possibility of contamination of the bacterial culture in the tank was minimized using aseptic techniques including autoclaving of the cell culture media and all other materials in contact with the culture, sealed operation of the culture tanks (except during billet removal), and use of sterile gloves and forceps when manipulating the billets. Due to their size, the tanks remained the incubator at 30°C throughout each experiment.

FLUORESCENT STAINING

A variety of methods may be used to distinguish between living and dead bacteria. One conservative indicator of bacterial mortality is the loss of bacterial membrane integrity (Korber et al., 1996). While a wide variety of stain pairs exist (Duffy and Sheridan, 1998; McFeters et al., 1995; Stewart et al., 1995; Williams et al., 1998), we chose the stain/counter-stain pair SYTO-16 and propidium iodide (PI) (both from Molecular Probes Inc., Eugene, Ore.). SYTO-16 stains all bacteria green by binding to nucleic acids. Propidium iodide also binds to nucleic acids, staining them a brilliant red. However, the molecular weight of PI is sufficiently large that it does not penetrate an intact bacterial membrane (Haugland, 1996). Thus, the nuclei of damaged bacteria appear red while all others appear green (Hood and Zottola, 1995). In this study, the optimal staining solution for biofilm visualization was a 1:5 ratio of 1 mM SYTO-16 in DMSO with 1 mg/mL PI in deionized water.

In the first group of experiments, sampling was performed at 24, 48, and 120 hours after the bacteria were added to the tank. In the second group, samples were taken for analysis at 24, 48, 96, and 144 hours. Three replicates were performed in the first group and two replicates were performed in the second group, for a total of five sets of data. From each tank, two billets of each material (G, PSS, and BSS) were removed using aseptic techniques and immersed in deionized water for 5 minutes to remove loose material. Next, 3 µl of the stain mixture PI/SYTO-16 was pipetted onto the biofilm, coverslipped (Corning, No. 1, Acton, Mass.), and incubated for 20 minutes in darkness. Two images (one each using the "FITC" and the "Rhodamine" filter packs) were taken at each of five random locations. The FITC filter passes light with a wavelength greater than 490 nm, allowing acquisition of cells fluorescing both red (PI) and green (SYTO-16). The Rhodamine filter passes light with a wavelength greater than 545 nm, allowing acquisition only of cells fluorescing red (PI). Thus, images captured with the FITC filter set include all of the cells, while those captured with the Rhodamine filter set include only non-intact cells.

IMAGE PREPARATION

Acquisition

A low-light black-and-white GBC-CCD video camera mounted on an epifluorescence microscope (Olympus, model BH2-RFCA, Lake Success, N.Y.) was used to obtain gray-scale images of the biofilms. Each image was captured at a resolution of 480×640 pixels and a depth of 256 levels of gray. The pixel size (0.349×0.349 µm) was determined using a stage micrometer at 20×. Digital image acquisition was performed on a Power Macintosh 8600 computer's internal frame grabber using the software package NIH Image (Rasband, 1999).

Noise Reduction, and Contrast Enhancement

Images acquired in very dim light, such as fluorescence, tend to include random background noise. The noise results from the fact that only a small number of photons are collected for each pixel. In our study, a series of 16 frames from the same location were averaged to reduce the noise that was present in the images (fig. 1). The acquisition times were sufficiently short (<5 seconds) that photobleaching of the fluorophores was not significant

(Russ, 1992). A 3×3 median filter was used for noise reduction. In this filter, the center pixel in the 3×3 neighborhood was replaced with the median value of the nine pixels, removing single-pixel noise. A number of methods have been developed for image analysis of bacteria (Lawrence et al., 1989; Lawrence et al., 1994; Yang et al., 2000). Since the biofilms that were used in our study fluoresce with different strengths depending on their substrate material, age, and the degree of photobleaching, automated thresholding was not practical; instead, manual thresholding was used.

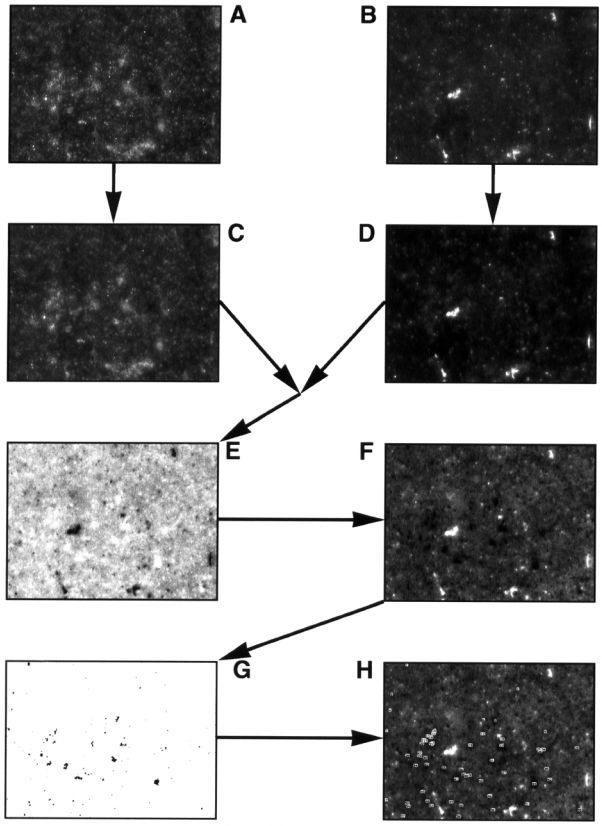

Figure 1. Steps of the image analysis process. Images A and B are the raw FITC and Rhodamine images, respectively. Images C and D are the enhanced FITC and Rhodamine images. Image E results from the subtraction and is inverted in F. Image F is then thresholded (G) and analyzed, and the individual patches are analyzed (H).

All of the images were contrast enhanced using histogram stretching. The histogram of a gray-scale image displays the number of pixels in the image having each of the 256 possible values of brightness. Peaks in the histogram correspond to the more common brightness values, while the valleys between the peaks indicate brightness values that are less common in the image. In most images, there are empty regions at either end of the histogram, indicating that the image brightness range does not cover the full 0-255 range available (Russ, 1998). Histogram stretching is the technique whereby the gray levels in the peak areas are spread out and the gray levels at the ends of the histogram, where no pixels exist, are removed. Thus, individual pixels retain their brightness order, but the values are shifted. Histogram stretching spreads out the values in regions where different regions meet, making it possible to identify minor variations within regions that appear nearly uniform in the original images. The features with brightness values below the selected threshold became part of the background, and the features above that value become part of the foreground. This normalization technique also brings the Rhodamine and FITC images onto the same scale, minimizing the differences due to fluorophore efficiency and optical transmissivity.

BIOFILM PATCH MORPHOLOGY

The individual *E. coli* growing on surfaces tend to aggregate in isolated groups or "patches." The morphology of these patches within a larger biofilm is an important factor to evaluate, since the response of the biofilm to attack from sanitizers and mechanical washing occurs at this level. For example, the effectiveness of a sanitizer is often limited by the characteristics of its diffusion into and reaction with the exopolysaccharide matrix. Therefore, there may be a substantial difference in the effectiveness of a sanitizer when a biofilm containing many small irregular patches is compared with one containing only a few large patches. Comparison of the patch morphology with morphology of the substrate may also allow identification of growth patterns that are related to the substrate, as opposed to those that are related to the bacterial strain.

Elimination of Dead Biofilm Patches

Our morphology analysis only considered undamaged biofilm patches. Image subtraction can be used to identify variations in images. In our process, the first of the two images contains all the bacteria (the FITC image) and the second only the dead bacteria (the Rhodamine image). The difference between these images includes only the living biofilm patches. To perform this subtraction, a Rhodamine image and an FITC images of the same location were individually enhanced and thresholded. Next, the pixel values from the Rhodamine image were subtracted from those of the FITC image, leaving only the intact biofilm patches. The resulting pixel values were then divided by two and added to 128 to re-center the pixel values within the 0 to 255 range. This image was contrast enhanced, thresholded, inverted (due to a limitation in NIH Image), and analyzed.

Morphometric Analysis

Three metrics were computed for the individual biofilm patches; patch area (*A*), patch perimeter (*P*), and circularity (*C*). Patches that touched the edge of the frame were not included in the analysis since they were not completely imaged. The size of the individual patches was determined using the number of pixels. The perimeters of the patches were calculated by counting the number of edge pixels and adding $\sqrt{2}$ for each corner pixel (Rasband, 1999). The areas and perimeters were exported to a spreadsheet (Excel, Microsoft Corp., Redmond, Wash.) and the patch circularities were calculated. Circularity is the ratio of the measured perimeter of a biofilm patch to the perimeter of a circle with the same area as the biofilm patch and is expressed as:

$$C = \frac{P}{2\sqrt{\pi \cdot A}} \quad (1)$$

where *P* is the perimeter and *A* is the area of the biofilm patch. A perfect circle has the circularity of 1, and other shapes have values for *C* greater than 1. By calculating the circularity of the patches grown on different materials, the effect of billet morphology and material, as well as the effects of the rinse in deionized water, can be evaluated (Russ, 1998). In future studies, the effectiveness of rinsing surfaces in a sanitizer versus water can be quantified by calculating and comparing the circularities. A biofilm growing on a rough surface such as brushed stainless steel is prone to primarily attach and grow in the crevices of the surface (Vanhaecke et al., 1990). The biofilm will therefore develop a more irregular shape, with a large circularity value, compared to a biofilm grown on a smooth surface such as polished stainless steel. The effect of a sanitizer would therefore vary depending on the surface. Polished stainless steel surfaces have also shown a larger resistance to cell attachment compared to a rough stainless steel surfaces (Arnold and Bailey, 2000). It has also been noted that biofilms from *E. coli* do not grow as well on glass as on stainless steel (Hyde et al., 1997).

BIOFILM COVERAGE OF THE SURFACE

Analyses of overall biofilm coverage and viability can be computed in two ways. In the first method, the coverage (in pixels) is compared with the available surface (640×480 pixels), and the average percent coverage of live and total biofilm is computed. In this approach, both the Rhodamine images (dead bacteria) and FITC images (all bacteria) were thresholded and their areas determined. If a biofilm merely dies from a treatment, but remains attached, then the surface may be more easily recolonized than a clean surface, which makes it important to look at the total coverage of biofilm, living and dead. In the second method, the percentage of intact or damaged biofilm is computed with respect to the total amount of biofilm.

STATISTICAL ANALYSIS

Each experiment was treated as a randomized complete block design with tanks as blocks. An analysis of variance (ANOVA) on the means was performed using SAS (SAS, 1999). Homogeneity of variance was checked using the criteria of Carroll and Ruppert (1988) for each variable. Patch areas, perimeters, and circularities were logarithmically transformed prior to the ANOVA analysis. The statistical level of significance throughout the analysis was 0.05. In order to avoid giving excessive weight to a few large biofilm patches, the medians of the total areas, perimeters, and circularities were also considered.

The analysis of the percent coverage for both groups of experiments included the fixed effects of material and time. Linear and quadratic interactions between areas over different sampling times were considered. Random effects included the tanks. The least significant difference test was used to examine the time-related effects. In the analysis of individual patch sizes on each material, a similar study was performed over individual areas, perimeters, and circularities of each patch of biofilm in every image. To avoid the possibility of pseudo-replication, a mean was calculated using the individual values of biofilm areas, based on replication and number of billets of the same material that were analyzed from each tank at each time. When the logarithmic transformation was required, this was performed prior to calculating the mean.

A linear regression analysis was performed, regressing the logarithm-transformed circularity against the logarithm-transformed area (Kuehl, 1994). As was true for the ANOVA analyses, the slope for the linear regressions was computed using the mean dependent and independent variable for each billet. The transformed circularities were regressed onto the transformed areas for the different materials in the two groups of experiments. With approximately the same number of biofilm patches per billet, the slope should be the same as the slope computed using individual values of biofilm patches. This greatly simplified the calculations and did not artificially inflate degrees of freedom associated with tests of significance. In order to investigate trends in growth on different materials, a linear regression was performed on the areas, perimeters, and circularities as a function of time. In addition, the medians of the areas, perimeters, and circularities for each material were analyzed. The medians in the first group of experiments were based on 32,200 data points (i.e., the number of biofilm patches where area, perimeter, and circularity was determined). The medians in the second group were based on 6,900 data points.

RESULTS AND DISCUSSION

PATCH MORPHOLOGY ANALYSIS

Our method for patch morphology is strengthened by its ability to distinguish biofilm patches containing undamaged bacteria from those that are damaged. In the future, this will allow us to establish whether surface features of the billets relate to the regions of effectiveness of various sanitizers or cleaning methods. The morphology analysis was performed on the median values of the areas, perimeters, and circularities (fig. 2). The decision to use the median values, instead of the means, was based on the presence of a few unusually large patches of biofilm. These large patches significantly altered the means. The medians gave information regarding the growth trends and shape of biofilms on different materials at different times.

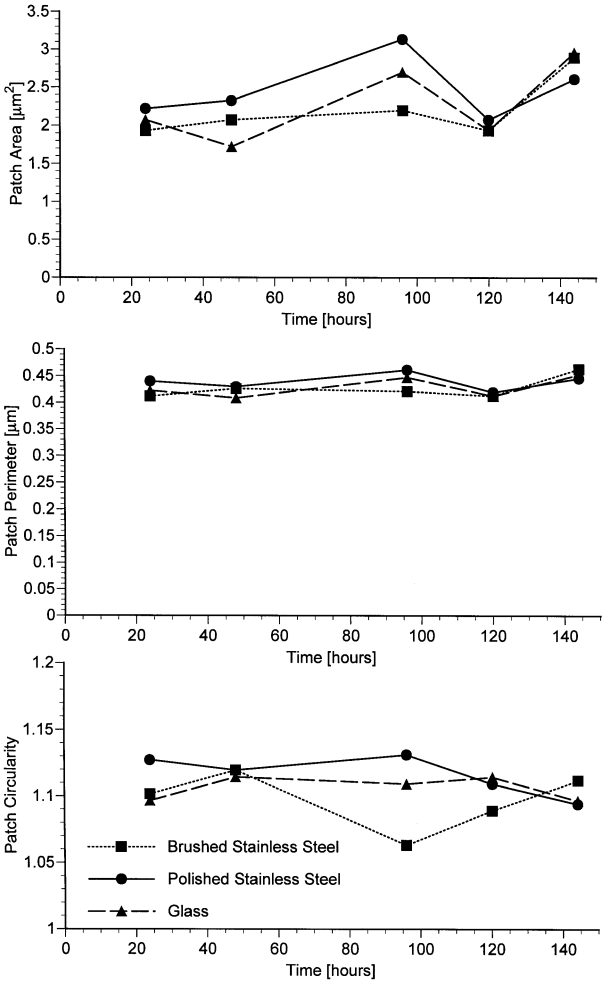

Figure 2. Medians of the areas, perimeters, and circularities for biofilms grown on glass, brushed stainless steel, and polished stainless steel. For each value of each median at each time, the three replications in group 1 and the two replications in group 2 are included.

Analysis of the Methodology

Color differentiation of cells obtained using dual staining is complicated by multiple factors. First, all of the cells are stained with one of the stains (in our case SYTO-16). However, a fraction of the cells is also stained with the second stain (in our case PI). The intensity of the light emitted from a stained cell can be affected by several factors including: the efficiency of the fluorophore, the affinity of the stain for the cellular component (i.e., the amount of fluorophores at the location), and the tendency of the fluorophore to bleach (Inoué, 1986). The intensity of the light at a given wavelength is also altered by the barrier filter, since the transmission is not uniform throughout the entire spectrum (Webster, 1978). Finally, CCD cameras are not uniformly sensitive across the entire spectrum (Van Vliet et al., 1998).

The second factor is "background" fluorescence. This can occur as the result of staining of various components within the culture medium, due to the leakage of intracellular components from disrupted bacteria or breakdown of the stain. Apparent background fluorescence can also occur as planktonic bacteria float across the field during acquisition of the multiple frames used in the frame-averaging process.

Both complications were adequately solved using the image enhancement techniques, especially the use of histogram stretching. The normalizing effect of the operation allowed clear differentiation of the stained cells from their surroundings. It also had the effect of minimizing slight variations in microscope adjustment and stain lots between the experiments. This simplified identification of consistent thresholds for a Rhodamine/FITC image pair

and allowed successful subtraction of the two images. However, when visually inspecting the images, variations in the biofilms' morphology could be identified. To investigate the shape of every individual patch, the perimeters also had to be estimated. Only with computer-based image analysis would this be possible for the 39,000 colonies and biofilm patches captured during this investigation.

Patch Area

The biofilms on the brushed stainless steel surfaces varied in $\log_{10}$ (patch area) between 0.975 and 1.55, the biofilms on polished stainless steel varied between 1.175 and 1.375, and the biofilms on glass varied between 1.1 and 1.3 (fig. 3). Apparently, the cells attached most quickly to a polished stainless steel surface, since the biofilm coverage on this surface was slightly higher than the biofilm coverage on a brushed stainless steel surface at the first sampling time (24 h). Both groups of experiments exhibited statistical differences in size of patch area depending on the material of the billet. The patch size also varied over time. In both groups, the area was different depending on whether the biofilm was grown on brushed stainless steel or glass. Only the second group showed a significant difference between BSS and PSS, while the first group indicated a small difference between G and PSS ($P < 0.06$). Group 2 indicated a clear linear change in area over time, while group 1 showed only a marginally significant change ($P < 0.06$).

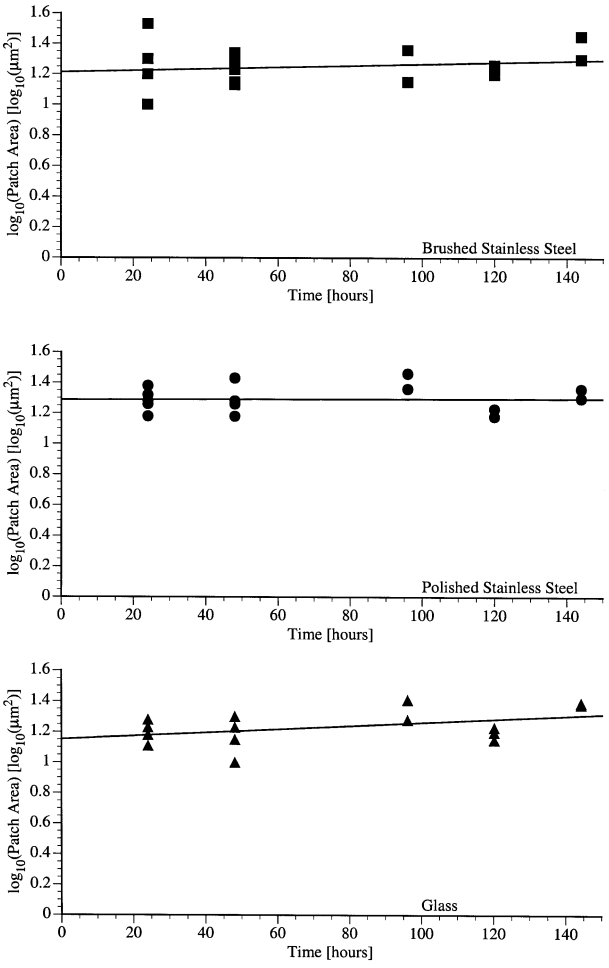

Figure 3. Regression lines for the mean of the logarithm-transformed values of the areas of the biofilms. The values are regressed on each time sampling of the biofilm that was performed. The mean of the transformed areas was calculated over material, time, replication, and billet. Each plot represents a different material.

Patch Perimeter

The perimeters of biofilm patches in the first group of experiments did not differ depending on the material upon which the biofilm was grown (fig. 4). In the second group, a small difference in perimeter was indicated between biofilms that were grown on BSS and PSS ($P < 0.05$). Both groups of experiments showed a clear difference in patch perimeters over time. When a linear regression was performed on the log-transformed perimeters, all of the intercepts were significantly different from zero. Only glass showed a slope significantly different from zero. The largest patch perimeter was found after 24 hours on polished stainless steel. Glass showed the smallest patch perimeter.

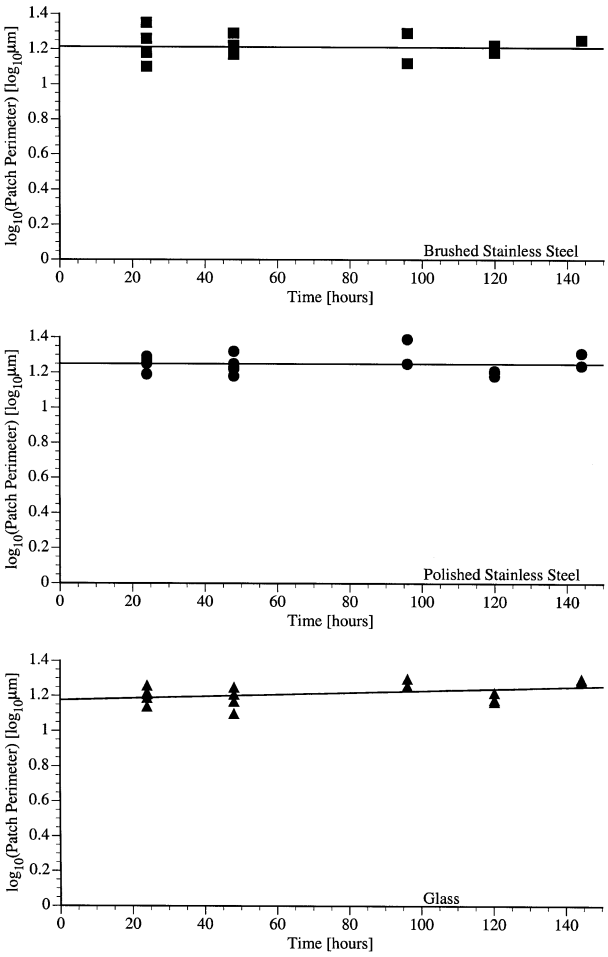

Figure 4. Regression lines for the mean of the logarithm-transformed values of the perimeters of the biofilms. The values are regressed on each time sampling of the biofilm that was performed. The mean of the transformed perimeters was calculated over material, time, replication, and billet. Each plot represents a different material.

Patch Circularity

One relationship between perimeter and area is circularity. When the circularities of the individual patches were computed, all the intercepts of the regression lines of circularity as a function of time were significantly different from zero (fig. 5). The brushed stainless steel and the glass had biofilms with similar circularities after 24 hours, while biofilms on the polished stainless steel had the largest circularity. However, by the end of each experiment, the circularity of biofilms on PSS had decreased to approximately the same values as circularities of biofilms on BSS and G. Only the polished stainless steel had a slope that was significantly different from zero, indicating that the circularity increased over time. Differences in circularity of the biofilm patches were found when grown on brushed

steel and glass in both groups of experiments ($P < 0.01$). In the first group, the circularity showed significant differences in behavior over time (using linear and quadratic models), while no changes over time were significant in the second group. Finally, the circularities of biofilms grown on glass and polished steel exhibited a very weak trend ($P < 0.08$).

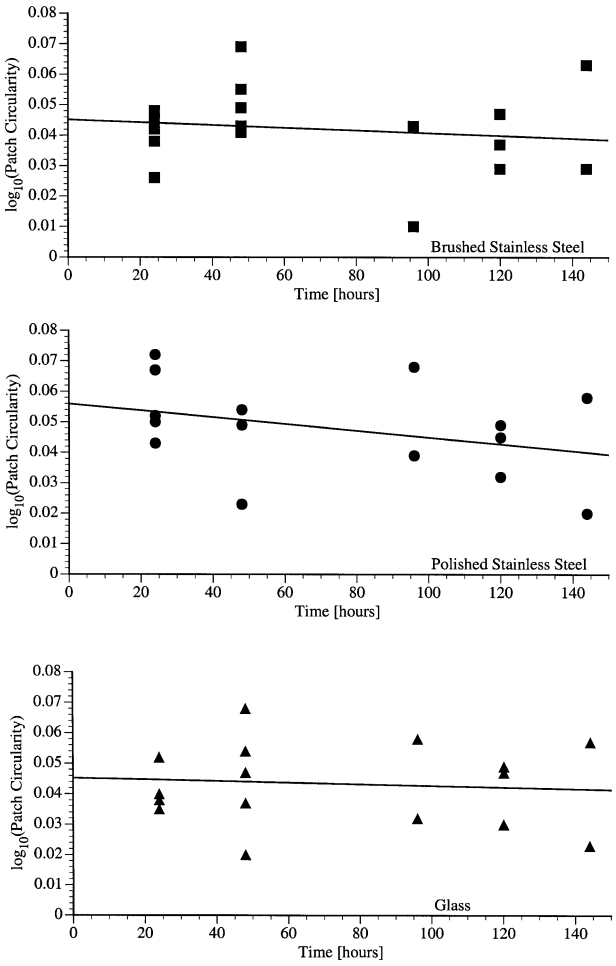

Figure 5. Regression lines for the mean of the logarithm-transformed values of the circularities of the biofilms. The values are regressed on each time sampling of the biofilm that was performed. The mean of the transformed circularity was calculated over material, time, replication, and billet. Each plot represents a different material.

Circularity and Area

One potential use for circularity is in examining the relationship between a patch's size and its shape. The log (circularity) was regressed with respect to the log (area) of biofilm. The groups of experiments were analyzed separately and were then merged and analyzed in aggregate. The common slope of the data in group 1 differed from one ($P < 0.01$) and indicated a weak deviation from that found in group 2 ($P < 0.06$). When groups 1 and 2 were merged, the slope did not deviate from one ($P < 0.18$).

Morphological Analysis Summary

The results indicate that *E. coli* K12 colonized a substrate quickly. On brushed and polished stainless steel, there were no significant increases in the size of the individual patches after 24 hours. We further noted that biofilm patches continued to increase in area on the glass billets over time (fig. 3). It is possible that this is the result of

slower colonization of the glass than of the stainless steel. A similar pattern is repeated when the perimeters are considered (fig. 4). Only on the glass do the colony perimeters increase.

Interestingly, when the circularities are computed, they remain essentially constant for the glass and the brushed stainless steel, but decrease for the polished stainless steel (fig. 5). However, it should be noted that the decrease in PSS circularity is from a value higher than the BSS and G circularities to a value similar to that of BSS and G. This counter-intuitive result occurs because circularity is a function of both the area and the perimeter. As a result, changes in the circularity occur only when the changes in patch area are not matched by appropriate changes in the perimeter.

The results suggest that the colonization of the *E. coli* K12 occurs within 24 hours. While the patch size is somewhat time dependent, it tends to approach a specific size. While the size of the patches stabilized, the shape of the biofilm patches continued to change. For example, the biofilm patches in this study tended to become more circular over time. Interestingly, while the growth patterns of these processes differ between glass and 316 stainless steel, they do not appear to differ in their steady-state values at 96 hours compared to 120 hours. Similarly, the eventual result of this biofilm growth seems unaffected by the surface characteristics of the stainless steel.

BIOFILM COVERAGE OF THE SURFACE

A typical analysis of biofilm coverage examines the percentage of the surface that is covered with the biofilm. In our research, the percentage coverage of biofilms with intact cells and total percentage coverage of biofilm with intact and damaged cell membranes was examined. Since the overall percentages of coverage are not location dependent, simply calculating the areas of each color was sufficient and more complex analysis methods were not necessary.

Each surface in our investigation showed large variations as a function of time and material (table 1). The glass seemed to have the smallest growth of biofilm, while brushed and polished stainless steel looked similar. Visual differences in percent biofilm coverage with respect to time could usually be seen. However, ANOVA showed no significant differences in the percentage of intact cells or the percentage of total cells in the biofilms with regard to either substrate or time ($P > 0.05$), nor was there a relationship between the material and time. There may be several reasons for this result. First, the biofilms were assumed to grow mainly in two dimensions. In addition, the biofilms may have reached the carrying capacity for each surface (i.e., the colonization and growth rates equaled the detachment and death rates). This is possible, since the staining of the 24-hour-old biofilms indicated that virtually all of the cell membranes were intact. However, after 96, 120, and 144 hours, the biofilms contained cells with disrupted cell membranes. It should be noted, however, that this system was examined only over relatively few days, and the strain of *E. coli* that was used is not known for producing substantial amounts of exopolysaccharide.

Table 1. Variation in percent biofilm coverage on three different materials at five different times. The two groups of experiments have been combined in this table.

% Bacteria with Intact Membranes				% Substrate Covered by Bacteria			
Time (h)	Glass (%)	Brushed Stainless Steel (%)	Polished Stainless Steel (%)	Time (h)	Glass (%)	Brushed Stainless Steel (%)	Polished Stainless Steel (%)
24	22-94	24-74	26-84	24	0.2-3.1	0.5-3.5	0.8-4.1
48	16-72	13-91	19-59	48	0.3-2.4	0.5-4.6	0.5-2.6
96	22-41	41-53	61-78	96	1.1-2.4	1.8-5.5	1.2-6.3
120	40-84	23-93	26-53	120	0.6-2.4	0.5-3.0	0.4-1.7
144	25-78	15-99	23-34	144	1.8-2.1	1.9-4.5	2.8-3.1

One notable aspect of this study was the small difference between the outcomes for highly polished stainless steel and stainless steel with a high degree of microscopic surface roughness. This result is consistent with that of Flint et al. (2000). One conclusion is that biofilms do not necessarily colonize stainless steel with a rough surface to a greater extent than that with a polished surface.

The percentage of biofilm growth may provide only limited strength as a tool for examining long-term biofilm growth. It will, however, allow the analysis of the early stages of biofilm growth and will allow comparison of techniques used to kill or remove biofilms, such as sanitizer or mechanical cleaning studies. The results of the analysis would likely be different for another bacteria strain. However, the analysis techniques are directly transferable for thin biofilms. In older, thicker biofilms, the thickness of the biofilm must also be considered.

Typically, information on the thickness is obtained using optical serial sectioning techniques on a confocal microscope. The techniques described in this research may be applied to each section prior to construction and analysis of the three-dimensional image.

CONCLUSIONS

We suggest a new tool for a rapid analysis of biofilms, using epifluorescence microscopy and image analysis. This tool allows the evaluation of overall biofilm coverage and biofilm patch morphology. Both methods are designed to distinguish between living and damaged bacteria. The coverage percentage allows evaluation of the growth of biofilms and will allow the evaluation of the effectiveness of sanitizers and mechanical cleaning methods in removing biofilms from food processing surfaces. The patch morphology is useful for investigating the relationships between surface morphology and biofilm growth and for determining the surface morphology, biofilm shape, and sanitizer effectiveness. Both analysis methodologies have been examined using biofilms grown from *E. coli* K12 on surfaces including polished stainless steel, brushed stainless steel, and glass.

ACKNOWLEDGEMENTS

The authors thank Dr. Jianhong Meng, Dept. of Nutrition and Food Sciences, University of Maryland, College Park, for the *E. coli* culture and for his advice and assistance in the study. We thank Linda Rinko and Kimberly Edwards, Dept. of Biological Resources Engineering, University of Maryland, College Park, for their assistance in the development of the staining protocols. The Maryland Agricultural Experiment Station and the College of Agriculture and Natural Resources, University of Maryland, College Park, funded this study.

REFERENCES

Arnold, J. W., and G. W. Bailey. 2000. Surface finishes on stainless steel reduce bacterial attachment and early biofilm formation: Scanning electron and atomic force microscopy study. *Poultry Sci*. 79(12): 1839-1845.

Camper, A. K., W. L. Jones, and J. T. Hayes. 1996. Effect of growth conditions and substratum composition on the persistence of coliforms in mixed-population biofilms. *Applied Environ. Microbiology* 62(11): 4014-4018.

Carnegie-Illinois. 1947. The fabrication of USS stainless and heat resistant steel. Pittsburgh, Pa.: Carnegie-Illinois Steel Corporation.

Carroll, R. J., and D. Ruppert. 1988. Transformation and weighting in regression In *Monographs on Statistics and Applied Probability*, 34. D. R. Cox, D. V. Hinkley, D. Rubin, and B. W. Silverman, eds. New York, N.Y.: Chapman and Hall.

Costerton, J. W., Z. Lewandowski, D. deBeer, D. Caldwell, D. Korber, and G. James. 1994. Biofilms: The customized microniche. *J. Bacteriology* 176(8): 2137-2142.

Danese, P. N., L. A. Pratt, and R. Kolter. 2000. Exopolysaccharide production is required for development of *Escherichia coli* K-12 biofilm architecture. *J. Bacteriology* 182(12): 3593-3596.

Dewanti, R., and A. C. Wong. 1995. Influence of culture conditions on biofilm formation by *Escherichia coli* O157:H7. *Int. J. Food Microbiology* 26(2): 147-164.

Duffy, G., and J. J. Sheridan. 1998. Viability staining in a direct count rapid method for the determination of total viable counts on processed meats. *J. Microbiol. Methods* 31(3): 167-174.

Escher, A. R., and W. G. Characklis. 1988. Microbial colonization of a smooth substratum: A kinetic analysis using image analysis. *Water Science and Technology* 20(11/12): 277-283.

Fletcher, M. 1996. *Bacterial Adhesion: Molecular and Ecological Diversity*. Wiley series in ecological and applied microbiology. New York, N.Y.: Wiley-Liss.

Flint, S. H., J. D. Brooks, and P. J. Bremer. 2000. Properties of the stainless steel substrate, influencing the adhesion of thermo-resistant Streptococci. *J. Food Eng*. (43): 235-242.

Haugland, R. 1996. *Handbook of Fluorescent Probes and Research Chemicals*. 6th ed. Eugene, Ore.: Molecular Probes, Inc.

Hood, S. K., and E. A. Zottola. 1995. Biofilms in food processing. *Food Cont.* 6(1): 9-18.

_____. 1997. Adherence to stainless steel by foodborne microorganisms during growth in model food systems. *Int. J. Food Microbiology* 37(2-3): 145-153.

Hyde, F. W., M. Alberg, and K. Smith. 1997. Comparison of fluorinated polymers against stainless steel, glass, and polypropylene in microbial biofilm adherence and removal. *J. Ind. Microbiol. and Biotech.* 19(2): 142-149.

Inoué, S. 1986. *Video Microscopy*. New York, N.Y.: Plenum.

James, G. A., L. Beaudette, and J. W. Costerton. 1995. Interspecies bacterial interactions in biofilms. *J. Ind. Microbiology* 15(4): 257-262.

Korber, D. R., A. Choi, G. M. Wolfaardt, and D. E. Caldwell. 1996. Bacterial plasmolysis as a physical indicator of viability. *Applied Environ. Microbiology* 62(11): 3939-3947.

Kuehl, R. O. 1994. *Statistical Principles of Research Design and Analysis*. Belmont, Calif.: Duxbury Press.

Kuehn, M., M. Hausner, H. J. Bungartz, M. Wagner, P. A. Wilderer, and S. Wuertz. 1998. Automated confocal laser scanning microscopy and semiautomated image processing for analysis of biofilms. *Applied Environ. Microbiology* 64(11): 4115-4127.

Kumar, C. G., and S. K. Anand. 1998. Significance of microbial biofilms in food industry: A review. *Int. J. Food Microbiology* 42(1-2): 9-27.

Lawrence, J. R., D. R. Korber, and D. E. Caldwell. 1989. Computer-enhanced darkfield microscopy for the quantitative analysis of bacterial growth and behavior on surfaces. *J. Microbiol. Methods* 10(2): 123-138.

Lawrence, J. R., G. M. Wolfaardt, and D. R. Korber. 1994. Determination of diffusion coefficients in biofilms by confocal laser microscopy. *Applied Environ. Microbiology* 60(4): 1166-1173.

Marshall, K. C. 1984. *Microbial Adhesion and Aggregatio.* Vol. 31. Life Sciences Research Report. Berlin, Germany: Springer-Verlag.

McFeters, G. A., F. P. Yu, B. H. Pyle, and P. S. Stewart. 1995. Physiological assessment of bacteria using fluorochromes. *J. Microbiol. Methods* 21(1): 1-13.

Rasband, W., NIH Image 1.62. Bethesda, Md.: National Institutes of Health.

Russ, J. C. 1992. *The Image Processing Handbook*. 1st ed. Ann Arbor, Mich.: CRC Press.

_____. 1998. *The Image Processing Handbook*. 1st ed. Ann Arbor, Mich.: CRC Press.

SAS. 1999. SAS version 6.12. Cary, N.C.: SAS Institute, Inc.

Sieracki, M. E., and C. L. Viles. 1998. Enumeration and sizing of micro-organisms using digital image analysis. In *Digital Image Analysis of Microbes: Imaging, Morphometry, Fluorometry, and Motility Techniques and Applications*, 175-196. M. H. F. Wilkinson and F. Schut, eds. New York, N.Y.: John Wiley and Sons.

Sternberg, C., B. B. Christensen, T. Johansen, A. Toftgaard-Nielsen, J. B. Andersen, M. Givskov, and S. Molin. 1999. Distribution of bacterial growth activity in flow-chamber biofilms. *Applied Environ. Microbiology* 65(9): 4108-4117.

Stewart, P. S., R. Murga, R. Srinivasan, and D. deBeers. 1995. Biofilm structural heterogeneity visualized by three microscopic methods. *Water Res.* 29(8): 2006-2009.

Tolker-Nielsen, T., U. C. Brinch, P. C. Ragas, J. B. Andersen, C. S. Jacobsen, and S. Molin. 2000. Development and dynamics of *Pseudomonas* sp. biofilms. *J. Bacteriology* 182(22): 6482-6489.

Van Vliet, L. J., F. R. Boddeke, D. Sudar, and I. T. Young. 1998. Image detectors for digital image microscopy. In *Digital Image Analysis of Microbes: Imaging, Morphometry, Fluorometry, and Motility Techniques and Applications*, 37-63. M. H. F. Wilkinson and F. Schut, eds. New York, N.Y.: John Wiley and Sons.

Vanhaecke, E., J. P. Remon, M. Moors, F. Raes, D. De Rudder, and A. van Peteghem. 1990. Kinetics of *Pseudomonas aeruginosa* adhesion to 304 and 316-L stainless steel: Role of cell surface hydrophobicity. *Applied Environ. Microbiology* 56(3): 788-795.

Webster, J. G. 1978. *Medical Instrumentation: Application and Design*. Boston, Mass.: Houghton Mifflin.

Wilkinson, M. H. F. 1998. Optical systems for image analyzed microscopy. In *Digital Image Analysis of Microbes: Imaging, Morphometry, Fluorometry, and Motility Techniques and Applications*, 65-89. M. H. F. Wilkinson and F. Schut, eds. New York, N.Y.: John Wiley and Sons.

Williams, S. C., Y. Hong, D. C. A. Danavall, M. H. Howard-Jones, D. Gibson, M. E. Frischer, and P. G. Verity. 1998. Distinguishing between living and nonliving bacteria: Evaluation of the vital stain propidium iodide and its combined use with molecular probes in aquatic samples. *J. Microbiol. Methods* 32(3): 225-236.

Wirtanen, G., and T. Mattila-Sandholm. 1993. Epifluorescence image analysis and cultivation of foodborne biofilm bacteria grown on stainless steel surfaces. *J. Food Prot.* 56(8): 678-683.

Yang, X., H. Beyenal, G. Harkin, and Z. Lewandowski. 2000. Quantifying biofilm structure using image analysis. *J. Microbiol. Methods* 39(2): 109-119.